Carbohydrate Research, 158 (1986) 191–204
Elsevier Science Publishers B.V., Amsterdam – Printed in The Netherlands

PROPERTIES OF XANTHAN GUM IN AQUEOUS SOLUTIONS: ROLE OF THE CONFORMATIONAL TRANSITION*

MICHEL MILAS AND MARGUERITE RINAUDO

*Centre de Recherches sur les Macromolécules Végétales (CERMAV-CNRS)**, B.P. 68-38402 Saint Martin d'Hères cedex (France)*

(Received September 16th, 1985; accepted for publication in revised form, May 1st, 1986)

ABSTRACT

Xanthan is shown to exist in native (I) and denatured (II) forms, both of which are ordered by the criterion of optical activity, and both of which undergo a temperature-driven, conformational transition to a common, disordered form (III). Changes in optical activity and conductivity are identical for the transformations I → III and II → III. The denatured, ordered form II displays a considerably larger viscosity increment than the native, ordered form I under given conditions of added salt at temperatures below the transition temperature (Tm). Light-scattering measurements yield the same molecular weight for forms I and II; consequently, the observed difference in viscosity increment appears to reflect inherent differences in the chain extension and conformation of forms I and II. Measured persistence lengths for forms I and II are consistent with earlier reports of the persistence length of single-stranded, ordered xanthan in solution. In the present viscosity studies, the absence of any dependence of measured properties of the native form I and the denatured form II on the thermal and concentration history strongly suggests that forms I and II are not aggregated species. Similar comparisons of the chain extension of disordered form III with the ordered forms I and II are more difficult, owing to the absence of conditions under which ordered and disordered forms are simultaneously stable. It is possible, nevertheless, to conclude that the viscosity increment of form II exceeds that of form III, whereas those of forms I and III are similar. Measurements of the molecular weight of form III, needed to convert this observation reliably into information about chain extension, are lacking. These observations are interpreted in terms of a model for xanthan in which the native, single-stranded, ordered form I is stabilized by side chain–backbone interactions that are shown, by experiments reported here, to be strong. These strong interactions are disrupted upon temperature-induced conversion into the disordered form III above the Tm. On subsequent cooling, there is established an alternative pattern of side chain–backbone interactions, presumably dictated by

---

*Presented at the Third European Symposium on Carbohydrates, Grenoble, September 16–20, 1985.

**Laboratoire associé à l'Université Scientifique Technologique et Médicale de Grenoble.

0008-6215/86/$ 03.50

kinetic rather than thermodynamic factors, which stabilizes a more-extended backbone conformation in the denatured, ordered form II. The assumption is made that these strong, side chain–backbone interactions can bridge some backbone breaks which can appear during partial degradation of forms I and II.

INTRODUCTION

Xanthan is the first bacterial polysaccharide to be produced on a large scale. It is an extracellular polysaccharide from the bacterium *Xanthomonas campestris*. Its solutions exhibit high viscosity with a pseudoplastic character. The main industrial use of xanthan gum is rheology control, such as in emulsion stabilization in the food industry or for reduction of the mobility of injected water in enhanced oil recovery. This polysaccharide in solution undergoes a thermal order–disorder conformational change widely studied by such spectroscopic methods as optical rotations, circular dichroism, and n.m.r.[1–4], and by viscosimetric or calorimetric measurements[1,5,6]

Some questions remain about the structure of the ordered conformation in aqueous solution. Self-association of xanthan molecules in aqueous solution has been demonstrated by Southwick *et al.*[7,8] from quasi-elastic light-scattering measurements. These intermolecular interactions can be suppressed in 4M urea as described by Dintzis *et al.*[9] and Frangou *et al.*[10], but Holzwarth and Prestridge[11] proposed a double-stranded helix on the basis of electron–microscopy observations, and then prepared denatured xanthan by heating for 15 min at 95°. By viscosimetry, light-scattering, or determinations of the sedimentation coefficient, Paradossi and Brant[12], Holzwarth[13], and Sato *et al.*[14] estimated the molar mass per unit contour length (M_L) of xanthan to be ~200 g/A in aqueous NaCl solution (using fractions of xanthan prepared by sonication). These authors concluded that the ordered conformation exists as a double strand. Moreover, Sato *et al.*[15] showed that, in cadoxen solutions, the xanthan behaves like a single, disordered chain with a ratio $\overline{M}_w$ (in 0.1M NaCl)/$\overline{M}_w$ (in cadoxen) of ~2, but, in aqueous solutions, other workers have demonstrated that, at least below 80°, the melting of the ordered transition does not lead to a dimer dissociation[6,16,17], and these authors proposed a single-stranded helix for the ordered conformation.

The aim of the present work was to present new information on the conformational transition, and to explain some consequences of the conformational transition on the properties of xanthan gum at temperatures <85°, where, in all cases, no interchain dissociation appears.

EXPERIMENTAL

Material. — To avoid problems connected with post-fermentation treatments, and also those arising from industrial preparation of dried xanthan powder, xanthan polysaccharide was obtained from Shell as an unpasteurized culture-broth.

The broth, which was never heated, was filtered through 0.45-μM Millipore filters, and precipitated from the filtrate with ethanol in M NaCl. The precipitate was rinsed with ethanol–water mixtures (50–90% EtOH, v/v) until no chloride ion could be detected potentiometrically in polymer solution prepared from the precipitate. Alternatively, the culture broth was centrifuged to remove cells, and ultrafiltered against 0.1M NaCl on Amicon XM 100 membranes to eliminate "small" molecules (such as proteins) and all ions except NaCl. To obtain samples without NaCl, the ultrafiltration was completed against distilled water. This procedure dispenses with all precipitation and drying steps. The xanthan concentration was determined by polymer precipitation, and the degree of hydration of the powdered precipitate was measured by thermogravimetry with a Setaram balance (Model G 70). Identical results were obtained with xanthan prepared by each of the two methods described. Xanthan in the calcium form was obtained either directly by ultrafiltration against $CaCl_2$ and then against water, or by adding $CaCl_2$ before precipitation and washing with ethanol–water mixtures. In all cases except ultrafiltration against water, the native xanthan conformation is preserved[18]. The pyruvic acetal and acetate contents are, respectively, 0.4 and 0.75, expressed as the average number of substituents per side chain. These were measured by using n.m.r. spectroscopy as described.

Certain xanthan samples were subjected to partial hydrolysis with mM oxalic acid containing 0.1M NaCl for 2 h at 90°. After neutralization of the acids, these samples were precipitated as already described and then redissolved in 0.01M NaCl for viscosity and optical rotation measurements. Throughout this procedure, the ordered xanthan conformation is preserved.

Techniques. — Viscosity measurements at low shear-rate limit were carried out by using a Contraves Low Shear LS 30 viscometer equipped with a Haake thermostat. For measurements above 35°, the viscometer and the solutions were separately heated at the desired temperature before pouring the solutions into the viscometer.

Intensities of light scattered from 0.01 and 0.1M aqueous NaCl solutions of Na xanthan at 25° were measured with a Fica 5000 light-scattering photometer in an angular range from 22.5 to 150° at 546 nm. The apparatus was calibrated with benzene. The Na xanthan solutions exhibited no polarization effect, and so no corrections were made for optical anisotropy. Because the extrapolation to zero angle is unsatisfactory due to the high radius of gyration, we used a low-angle laser light-scattering apparatus (Chromatix KMX 6) to measure the scattered intensities at 6° of a 0.025 g/L xanthan in 0.01 or 0.1M NaCl solution. All the points allow drawing of the Zimm plot and deducing of the weight average molecular weight and the average radius of gyration. Optical clarification of xanthan solutions was achieved by filtration through 0.22-μm Millipore filters.

The specific refractive index increment was determined by using a Brice–Phoenix differential refractometer. The value of dn/dc obtained was 0.155 (mL/g) in 0.01 and 0.1M NaCl solutions without dialysis. Optical rotation at 300 nm was determined by using a Fica Spectropol 1b instrument with a 5-cm quartz cell thermostated with a Haake thermostat.

^{1}H-N.m.r. measurements were conducted with a Bruker WP 100 spectrometer, with suppression of OH signals by irradiation; 200 scans were accumulated, with a repetition time of 7 s and a sweep width of 1125 Hz. Dried xanthan was dissolved in 5mM sodium acetate solution in D_2O at a polymer concentration of ~5 g/L. Sodium acetate was used as the internal standard for determination of the degrees of pyruvation and acetylation.

Conductances of Na xanthan solutions were determined by using a Tacussel CD 78 conductimeter. For measurements as a function of temperature, we recorded the ratio (R) between the conductance of the xanthan solution and that of a NaCl solution having the same initial conductance at 25°. By using cells with the same constant, this ratio is quasi-independent of the variation of the conductance with the temperature, and shows the influence of the conformational transition on the xanthan conductance.

RESULTS AND DISCUSSION

A. Viscosimetric evidence for two ordered conformations. — When the native xanthan is heated, it undergoes a conformational transition that depends on the concentration of added salt, as previously described[2,3]. This transition is usually observed with optical activity measurements, as shown in Fig. 1a, where the specific rotation at 300 nm is plotted *versus* temperature T for a series of salt concentrations. For all of the salt concentrations studied, measurements of $[\alpha]_{300}$ *versus* T are independent of whether T is increasing or decreasing. The temperature, T_m, corresponding approximately to the temperature where the slope of the plot of $[\alpha]_{300}$ *versus* T is greatest, is a characteristic "melting" temperature for the transition that

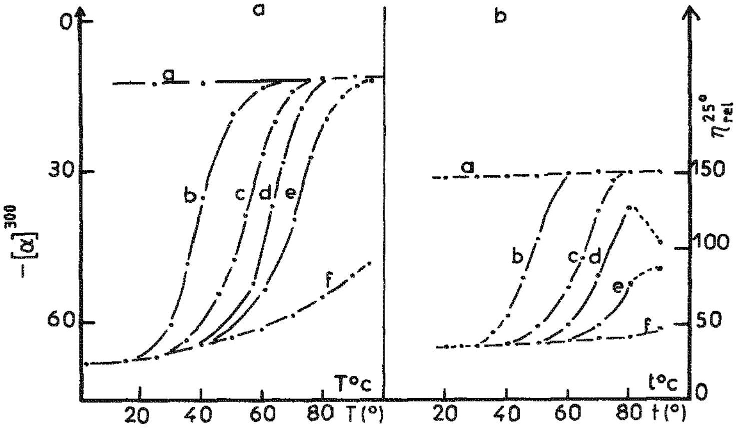

Fig. 1. a. Specific optical rotation as a function of temperature T for Na xanthan. [C_p = 0.66 g/L, in a, H_2O; b, 5.6mM NaCl; c, 10.8mM NaCl; d, 15.8mM NaCl; e, 28mM NaCl; and f, 0.1M NaCl]. b. Relative viscosity in the lower Newtonian region for the different xanthan solutions (see Fig. 1a) at T = 25° and 0.1M NaCl, after preheating at different temperatures t and NaCl concentrations.

clearly depends on the concentration of added salt. The form present at low temperature (large absolute $[\alpha]_{300}$) is usually said to be in an "ordered" conformation, whereas the high temperature plateau in $[\alpha]_{300}$ corresponds to the "disordered" form.

It is of interest also to monitor the transition by using viscosity measurements, in order to obtain more-direct information about the macromolecular conformation. In Fig. 1b are reported measurements of the relative viscosity (η_{rel}) in the lower Newtonian regime of a xanthan solution at a concentration of 0.66 g/L. These measurements were all made at 25° in 0.1M NaCl solution following heating of the xanthan solution to a predetermined temperature t under the several conditions of added salt described in Fig. 1a. For these experiments, a 5-mL xanthan solution at the desired salt concentration was heated to some constant temperature t in a thermostat bath, and later returned to 25°; the NaCl concentration was then adjusted to 0.1M prior to the measurement of η_{rel}. The measured η_{rel} proved to be independent of the time for which the sample was held at the elevated temperature, the subsequent rate of cooling to 25°, and the time intervening before the measurement of η_{rel}. The standard conditions chosen for measuring η_{rel} permitted comparison of conformational differences in the preheated xanthan samples under conditions where the electroviscous contributions to η_{rel} are small and are effectively the same for all of the sample. The standard conditions correspond, for all of the xanthan samples, to the ordered state of the polymer, as disclosed by optical activity measurements.

It is clear from Figs. 1a and 1b that, for the lower salt-concentrations (curves b and c), there is a strong correlation between η_{rel} measured under standard conditions and $[\alpha]_{300}$. That is, the higher the preheating temperature and, thus the greater the degree of conformational disorder (measured at that temperature and salt concentration by $[\alpha]_{300}$), the larger the measured η_{rel}. Because the optical activity curves (Fig. 1a) are reversible and, under the standard conditions for measuring η_{rel}, the samples have regained their original values of $[\alpha]_{300}$ prior to heating, it may be concluded that, as disclosed by η_{rel}, the ordered polymer has a different conformation before and after heating. These observations suggest the existence of three conformational states for xanthan: I, the native, ordered form (never heated); II, the denatured, ordered form (heated to T_m or above, and then cooled); III, the disordered form (present at high temperature or low salt concentration, or both). At the higher salt concentration (curves d and e), the correlation of η_{rel} and $[\alpha]_{300}$ does not persist for t >80°, which suggests a partial recovery of form I when the disorder-to-order transition occurs at higher temperature.

In Fig. 2 are shown measurements of η_{rel} as a function of temperature T for xanthan at 0.66 g/L and at a NaCl concentration of 0.1 and 0.01M; in this case, η_{rel} is measured at the temperature T and salt concentration specified, not under the standard conditions previously described. The corresponding plots of $|[\alpha]_{300}|$ *versus* T are shown as dashed lines in the Figure as well; the latter curves are identical under given conditions of NaCl concentration for ordered forms I and II, as re-

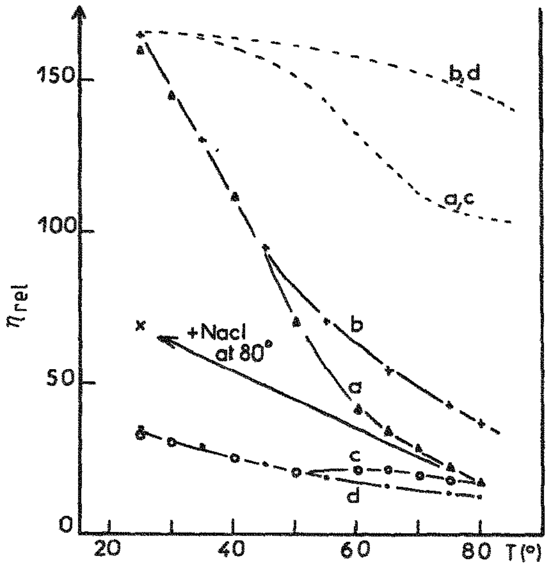

Fig. 2. Relative viscosity in the lower Newtonian region for xanthan as function of the temperature. ▲: from II in 0.01M NaCl (a), +: from II in 0.1M NaCl (b), ○: from I in 0.01M NaCl (c) and ●: from I in 0.1M NaCl (d). Dashed line: optical rotary power variation with temperature for these solutions. ×: relative viscosity restored at 25° when NaCl is added at 80° into a III form xanthan solution (see text).

quired by the reversibility of the data in Fig. 1a. Curves a (0.01M NaCl) and b (0.1M NaCl) correspond to xanthan which has been thermally denatured. Thus, at low T, it is in form II and passes in 0.01M NaCl to form III at high T along curve a, as T_m = ~58° (at this salt concentration). At 0.1M NaCl, the T_m is >100°, and so the chiroptically detected, conformational transition does not occur along curve b. Under these conditions of molecular weight, polymer concentration, and salt concentration, form II displays a larger η_{rel} than does form III at 80°. Both viscosity curves (a and b) are thermally reversible. Curves c (0.01M NaCl) and d (0.1M NaCl) correspond at low T to the native, xanthan form I. At the higher salt concentration, η_{rel} decreases with increasing T, without a conformational transition; viscosity curve d is thus thermally reversible. On the other hand, viscosity curve c diverges from curve d near T = 50°, and moves to join curve a at 80°, where form III exists. Cooling of form III from 80° at 0.01M NaCl always follows curve a, and, viscosity curve c is, therefore, not reversible. It should be noted that, under the conditions of these experiments, form III has a larger η_{rel} than has form I at 80°, but this comparison is not at the same salt concentration, and so the meaning of this observation is somewhat unclear.

Of greatest significance is the fact that η_{rel} for the denatured, ordered form II is always substantially greater than that for the native, ordered form I at all temperatures (curves b and d). The two ordered forms, however, melt to the same disordered form, III, when T is sufficiently greater than T_m (curves a and c). When NaCl is added to form III in 0.01M NaCl at 80°, to raise the salt concentration to

0.1M and thus increase T_m to ~100°, the disordered-to-ordered transition is induced to occur at 80°. Cooling this solution to 25° then yields η_{rel} intermediate between the values on curves b and d, suggesting again that, when the disorder-to-order transition occurs at high enough temperature, form I is partially recovered on cooling.

Relative viscosities in the low Newtonian region have been measured as a function of temperature and polymer concentration from 0.0125 to 0.200 g/L. The corresponding, reduced specific viscosities have been extrapolated to vanishing concentration at each temperature, to yield the intrinsic viscosities $[\eta]$ shown in Fig. 3. Curves a (0.01M NaCl) and b (0.1M NaCl) correspond at low T to form II. Curves c (0.01M NaCl) and d (0.1M NaCl) refer at low T to form I. Form III exists above 70° on curves a and c. Below 50°, all four intrinsic-viscosity curves decline with increasing T, with a temperature coefficient dln $[\eta]$/dT of about -0.008 deg^{-1}. The order-to-disorder conformational transition in form II (curve a) leads to a still larger temperature coefficient for this form in the temperature range of the transition above 50°. On the other hand, the effect of the transition on the temperature dependence of $[\eta]$ for the native, ordered form I is scarcely perceptible and, if anything, is to reduce the magnitude of the temperature coefficient (curve c). As was evident also from the relative viscosities in Fig. 2, the denatured, ordered form II produces a larger viscosity increment than does the native, ordered form I at all temperatures, but both forms melt to a common, disordered form III which, at 80°, has a hydrodynamic volume at 0.01M NaCl larger than that of form I at 0.1M NaCl and smaller than that of form II at 0.1M NaCl.

The magnitude of the temperature coefficient dln $[\eta]$/dT below 50° may be

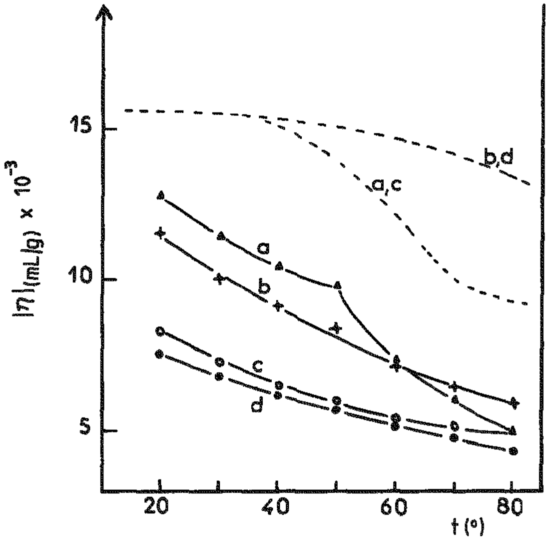

Fig. 3. Intrinsic viscosity variation with temperature for the four xanthan solutions (see Fig. 2). Dashed line: optical rotation variation with temperature for these solutions.

compared with the range -0.007 to -0.008 deg^{-1} observed for other cellulosic chains[19,20]. Consequently, except in the conformational transition temperature range above 50° (curves a and c), this coefficient is the same for xanthan. The fact that this coefficient is far more sensitive to the conformational transition in form II than in form I may provide an important clue to the difference between these two ordered form. A difference in this coefficient, in comparison with other cellulosic chains, would also be expected if the xanthan ordered states were a double-stranded helix.

The dependence of η_{rel} on polymer concentration C_p is given at 25° in 0.1M NaCl. The relative viscosity of the denatured, ordered form II depends more strongly on C_p, as anticipated from the foregoing results. Under these conditions of temperature, molecular weight, and salt concentration, the respective, overlap concentrations $C_p{}^*$ of forms I and II are ~0.13 and 0.09 g/L. It may be concluded, as already evident from the intrinsic viscosity results, that the larger relative viscosity of form II persists into the dilute solution regime, and is not a consequence simply of dominant intermolecular interactions present at higher concentration in the denatured, ordered state. This is an important result in support of our earlier contention[16] that the order-to-disorder transition in xanthan is an intramolecular process.

If the native ordered form were double stranded[12,15,21] the denatured, ordered species II might be expected to be a partially reassociated form, of less-perfect order, containing some aggregates with more than two chains per aggregate and having impaired single-strand segments capable of associating with similar, single strands from other aggregates. This behavior does not need a complete, dimer dissociation of the double strands in the form III; but, on the contrary, we have shown that the larger viscosity increment of form II persists into the dilute solution regime, and may thus be reasonably attributed to the greater extension (hydrodynamic volume) of the denatured, ordered molecules in form II. Molecular-weight measurements, reported in Table I, serve to support this contention.

We note finally, with reference to Figs. 1–4, that the results of our measurements on form II do not depend, once form II has been properly prepared at relatively low salt concentration, on its thermal or concentration history. The data for form II in Fig. 4, for example, can be reproducibly obtained by heating solutions

TABLE I

RESULTS FROM LIGHT SCATTERING AND VISCOSITY OF Na XANTHAN SAMPLES IN 0.1M AQUEOUS NaCl

Form	$\overline{M}_w$	$[\eta]$ $(mL \cdot g^{-1})$	*Rg* *(Å)*	q^a *(Å)*	q^b *(Å)*
I	7.0×10^6	7100	3100	290	400
II	6.5×10^6	10,600	3900	410	730

[a] Persistence length from Eq. *1*. [b] From Eq. *2*.

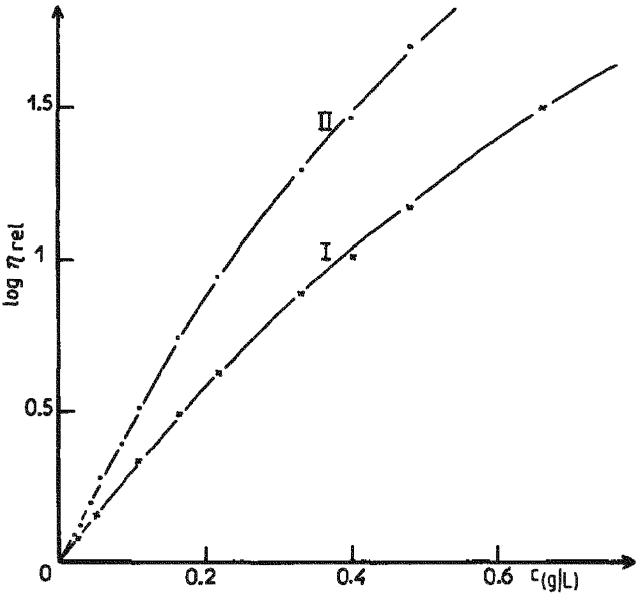

Fig. 4. Relative viscosity in the lower Newtonian region as function of xanthan concentration for forms I and II at T = 25°: in 0.1M NaCl.

of form I over a wide range of polymer concentrations (0.055 to 15 g/L) at 0.01M ionic strength (taking into account the xanthan contribution) and by diluting the resulting form II at 0.01M NaCl, regardless of the polymer concentration at which it was prepared, to the desired polymer concentration. The reproducibility of these measurements on form II, irrespective of thermal and concentration history, militates against its being an aggregated form.

B. Conductance measurements. — Information about the chain conformation and linear charge density of a polyelectrolyte may be obtained from conductance measurements[22]. In Fig. 5 are reported data on the conductance of native and denatured xanthan as a function of temperature at a xanthan concentration (C_p) of 15 g/L in pure water. Under these conditions of high polymer concentration, the ionic strength due to the polyelectrolyte alone is large enough to cause T_m ~55° in the absence of added salt. Other experiments at C_p = 1 g/L in 0.01M NaCl, where also T_m ~55°, yield essentially identical conductimetric results. The data in Fig. 5 correspond to the ratio R of the conductance of the polymer solution to that of a NaCl solution having the same conductance at 25°; presentation of the data in this form removes most of the trivial temperature-dependence of the conductivity of salt solutions, and serves to emphasize the effect of the conformational transition.

Forms I and II show a very similar T dependence of R. The conformational transition is accompanied in the temperature range of 40 to 70° by an 11% increase in conductance. A 9% conductance increase is predicted, using Manning's theory[23], by assuming a change in the charge density parameter corresponding to a backbone

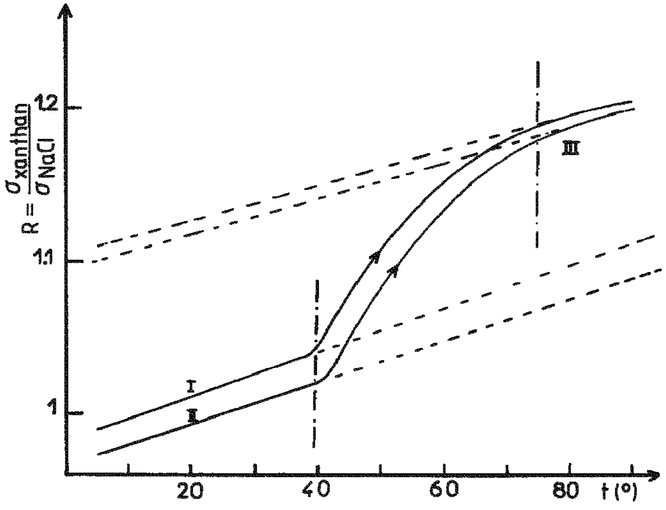

Fig. 5. Variation of the conductance ratio R between xanthan solution C_p = 15 g/L and NaCl solutions with the same conductance at 25° as function of the temperature for the initial ordered conformations I and II (see text).

conformational change from a single-stranded 5_1 helix to the fully extended chain[5,6], and by assuming that the conductance is insensitive to any conformational change accompanying the transition.

C. Chain characteristics. — Treating xanthan as a wormlike chain, we have estimated the persistence length $q = \frac{1}{2}\lambda$ of ordered forms I and II from $[\eta]$, using the Yamakawa–Fuji theory[24] and Eq. *1*.

$$\frac{1}{\lambda} = \frac{([\eta] \cdot M_L^{3/2})^{2/3}}{M^{1/2} \cdot \Phi_{(L,d)}}, \qquad (1)$$

where M_L = 100 g/Å is the assumed mass per unit length, d = ~20Å is the assumed diameter of the chain, $L = \overline{M}_w/100$ is the contour length, M is the weight average molecular weight, and $\Phi_{(L,d)}$ is a function of L and d; its values are given in ref. 24.

The persistence length has also been estimated from the light-scattering radii of gyration R_G, using the relationship in Eq. *2* of Benoit and Doty[25] applicable to wormlike chains.

$$R_G^2 = L^2[1/3x - 1/x^2 + 2/x^3 - 2/x^4 (1 - e^{-x})], \qquad (2)$$

where $x = L/q$. The results for q calculated from Eqs. *1* and *2* are given in Table I, along with the measured values of $\overline{M}_w$, $[\eta]$, and R_G for forms I and II at 25° in 0.1M NaCl. The values of q from light-scattering and viscosity are in reasonable agreement for each ordered form, provided that it is recognized that the samples were not fractionated ($\overline{M}_w/\overline{M}_n$ = ~1.4 from g.p.c. measurements with light-scattering detection of the MWD). The transition from I to II corresponds to a small increase in chain extension. The values of q obtained are consistent with the value q = ~500 A reported for single-stranded xanthan by Muller *et al.*[26]. Larger values of q (1000–1500 A) have been reported for other xanthan samples produced by Kelco[15,21], and believed by the authors to correspond to a double-stranded form of xanthan[5,11–15,21]. The near-identity of $\overline{M}_w$ measured for forms I and II in this work strongly suggests, however, that the denatured, ordered form II does not represent a reassembled, double-stranded structure from a fully or partially dissociated native double-stranded form.

D. Existence of stabilized, backbone breaks. — Experiments with partially depolymerized xanthan suggested that strong interactions of the side chains with the backbone can even mask the existence of cleavage in the covalent structures of the backbone. For these experiments, ordered xanthan (form I or II) was subjected to acid, thermal, enzymic, or ultrasonic depolymerization, and then experimental samples were prepared by precipitation as described in the Experimental section. When η_{rel} was measured for these samples, in an experiment parallel to that described in Fig. 1b, the results shown by the solid curve of Fig. 6 were found. In this case, ordered xanthan form II was depolymerized by acid hydrolysis as described in the Experimental section. The xanthan was dissolved at C_p = 0.6 g/L, and heated to predetermined temperature t at 0.01M NaCl before measurement of η_{rel} under standard conditions.

For the first cycle of heating (curve a), the η_{rel} measured under standard conditions declines as the temperature to which the sample has been preheated is increased, in sharp contrast to Fig. 1b. For samples that have once been heated above 80°, η_{rel} (measured again under standard conditions following preheating to temperature t) follows curve b. Thus, curve b can be repeated time and again with a given sample, whereas curve a cannot, once the sample has been heated to 80°. The dashed curve in Fig. 6 described the dependence of $[\alpha]_{300}$ on T; it is reversible,

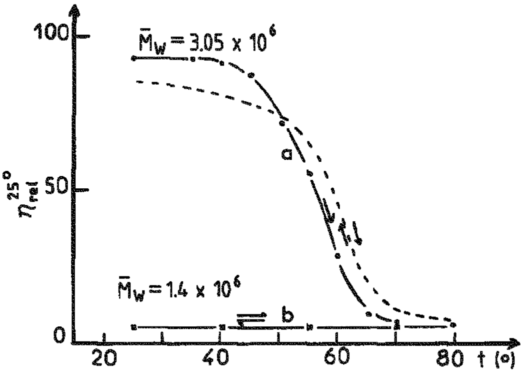

Fig. 6. Relative viscosity at low shear rate limit versus the preheating temperature for an initially degraded xanthan in form II. a: irreversible process during the first preheating beyond T_m; b reversible process after the first preheating. C_p = 0.6 g/L in 0.01M NaCl; T = 25°. Dashed line: the optical rotation variation with temperature for these solutions (a,b).

and corresponds to both viscosity curves a and b. The initial molecular weight of this sample, prior to the initial heating, was 3.05×10^6; a value about half this large characterizes the sample after it has been heated to 80°. These results are not restricted to samples hydrolyzed with acid, but are found equally for samples partially depolymerized by the order methods mentioned, and, sometimes, in native, ordered form I. This behavior can be used to explain the small difference between $\overline{M}_w$ of the forms I and II (see Table I).

We explain the foregoing observations by postulating that some of the points of covalent rupture in the backbone are initially masked by strong sidechain–backbone interactions which are disrupted on passing through the temperature-driven, order-to-disorder transition and are not re-established on subsequent cooling. We exclude the possibility that drop in η_{rel} corresponds to dissociation of double-stranded dimer, by noting that the conductance, and here the linear charge-density of the chain, is the same for the partially depolymerized samples before and after they are heated past T_m. The drop in η_{rel} at T_m is thus attributed to dissociation of the "end-to-end aggregates" held together initially by strong sidechain–backbone interactions.

CONCLUSIONS

In this work, we have shown that xanthan may exist in two different conformations, both of which are "ordered" as judged by optical activity measurements. Heating of native, ordered xanthan (form I) beyond the transition temperature T_m produces the disordered form III, which, upon cooling, leads to the denatured, ordered form II. The magnitude and variations of the optical rotation and the conductance, *i.e.*, the charge density of the xanthan chain, are identical for the transformations I → III and II → III. States I and II exhibit different viscosities in solution, but display no difference in molecular weight in the absence of prehydrolysis of polymer backbone. The results reported here for Na xanthan are also found for Ca xanthan, although T_m is so high in the latter case ($T_m > 100°$) that form III is never observed.

We interpret these results in terms of worm-like, single-stranded molecules for both of the ordered conformations. The denatured, ordered form II is more extended than the native, ordered form I. We consider that the differences in conformation involve a rearrangement of the pattern of sidechain–backbone interactions, which, our studies of partially hydrolyzed xanthan suggest, are very strong indeed. Thus, passage from the native form I to the disordered form III is presumed to involve disruption of the native pattern of sidechain–backbone interaction. On cooling, this pattern is not re-established, and the denatured form displays a different pattern of interactions that stabilizes a more-extended backbone conformation. Form II may not be thermodynamically more stable than form I; evidence that form I may be re-established on cooling of form III, if the disorder-to-order transition occurs at a high enough temperature, suggests that form II is trapped by

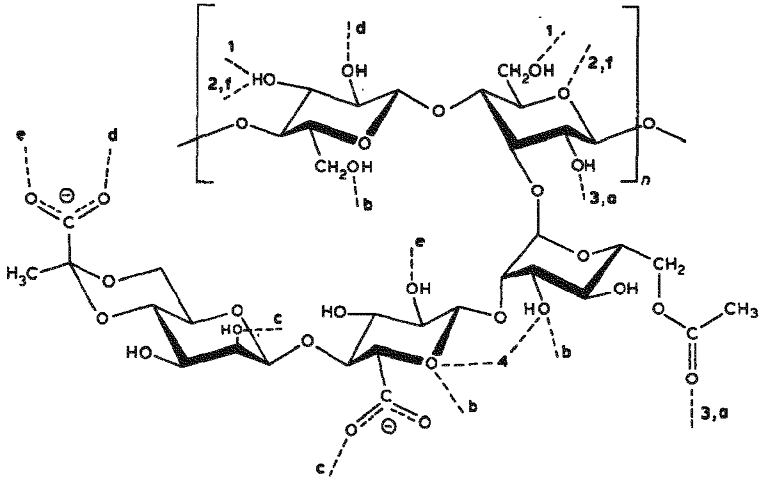

Fig. 7. Possible hydrogen bonds in xanthan molecules. Some adjoining residues involves in hydrogen bonds are omitted for clarity and the positions of residues are speculative; a–f[27]; 1–4[28].

kinetic factors in a thermodynamically less-stable state. Some speculations about the possible patterns of sidechain–backbone interactions in forms I and II are presented in Fig. 7. Little information is available about form III. We presume it to be a single-stranded, random coil in which the importance of sidechain–backbone interactions is greatly diminished. It appears certain that, if forms II and III could be compared under identical conditions of temperature, solvation, and ionic strength, form II would be found to be considerably more extended than form III. This is implicit in the large temperature coefficient $d\ln[\eta]/dT$ observed for the transformation II → III above 50° in Fig. 3. On the other hand, the small temperature coefficient for the transformation I → III suggests that form III might be as extended as, or even more extended than, form I at 80° in 0.01M NaCl. Unfortunately, a molecular-weight detemination of form III is not at present available.

ACKNOWLEDGMENTS

The authors thank Shell Research, Ltd., for the sample of xanthan broth, Dr. Clarke-Sturman for helpful discussions, and Dr. D. A. Brant for his critical reading of this manuscript and his valuable comments.

REFERENCES

1 E. R. Morris, D. A. Rees, G. Young, M. D. Walkinshaw, and A. Darke, *J. Mol. Biol.*, 110 (1977) 1–17.
2 G. Holzwarth, *Biochemistry*, 15 (1976) 4333–4339.
3 M. Milas and M. Rinaudo, *Carbohydr. Res.*, 76 (1979) 189–196.
4 M. Rinaudo, M. Milas, F. Lambert, and M. Vincendon, *Macromolecules*, 16 (1983) 816–819.
5 S. Paoletti, A. Cesaro, and F. Delben, *Carbohydr. Res.*, 123 (1983) 173–178.
6 I. T. Norton, D. M. Goodall, S. A. Frangou, E. R. Morris, and D. A. Rees, *J. Mol. Biol.*, 175 (1984) 371–394.

7 J. G. Southwick, H. Lee, A. M. Jamieson, and J. Blackwell, *Carbohydr. Res.*, 84 (1980) 287–295.
8 J. G. Southwick, A. M. Jamieson, and J. Blackwell, *Carbohydr. Res.*, 99 (1982) 117–127.
9 F. R. Dintzis, G. E. Babcock, and R. Tobin, *Carbohydr. Res.*, 13 (1970) 257–267.
10 S. A. Frangou, E. R. Morris, D. A. Rees, R. K. Richardson, and S. B. Ross-Murphy, *J. Polym. Sci., Polym. Lett. Ed.*, 20 (1982) 531–538.
11 G. Holzwarth and E. B. Prestridge, *Science,* 197 (1977) 757–759.
12 G. Paradossi and D. A. Brant, *Macromolecules,* 15 (1982) 874–879.
13 G. Holzwarth, *Carbohydr. Res.*, 66 (1978) 173–186.
14 T. Sato, T. Norisuye, and H. Fujita, *Macromolecules,* 17 (1984) 2696–2700.
15 T. Sato, T. Norisuye, and H. Fujita, *Polym. J.*, 16 (1984) 341–350.
16 M. Rinaudo and M. Milas, *Biopolymers,* 17 (1978) 2663–2678.
17 I. T. Norton, D. M. Goodall, E. R. Morris, and D. A. Rees, *J. Chem. Soc., Chem. Commun.*, (1980) 545–547.
18 M. Milas and M. Rinaudo, *Polym. Bull.*, 12 (1984) 507–514.
19 P. J. Flory, O. K. J. Spurr, and D. K. Carpenter, *J. Polym. Sci.*, 27 (1958) 231–240.
20 D. W. Tanner and G. C. Berry, *J. Polym. Sci., Polym. Phys. Ed.*, 12 (1974) 941–975.
21 T. Sato, S. Kojima, T. Norisuye, and H. Fujita, *Polym. J.*, 16 (1984) 423–429.
22 C. Rochas and M. Rinaudo, *Carbohydr. Res.*, 105 (1982) 227–236.
23 G. S. Manning, in E. Selegny (Ed.), *Polyelectrolytes,* Vol. 1, Reidel, Dordrecht, Holland, 1974, pp. 9–37.
24 H. Yamakawa and M. Fujii, *Macromolecules,* 7 (1974) 128–135.
25 H. Benoit and P. Doty, *J. Phys. Chem.*, 57 (1953) 958–965.
26 G. Muller, J. Lecourtier, G. Chauveteau, and C. Allain, *Makromol. Chem., Rapid Commun.*, 5 (1984) 203–208.
27 R. Moorhouse, M. D. Walkinshaw, and S. Arnott, in P. A. Stanford and A. I. Laskin (Eds.), *Extracellular Microbial Polysaccharides, A.C.S. Symp. Ser.*, 42 (1977) 90–102.
28 K. Okuyama, S. Arnott, R. Moorhouse, M. D. Walkinshaw, E. D. T. Atkins, and C. Wolf-Ullish, in A. D. French and K. H. Gardner (Eds.), *Fiber Diffraction Methods, A.C.S. Symp. Ser.*, 141 (1980) 411.